Lia A. Moulopoulos, MD • Datla G. K. Varma, MD • Meletios A. Dimopoulos, MD
Norman E. Leeds, MD • E. Edmund Kim, MD • Dennis A. Johnston, PhD
Raymond Alexanian, MD • Herman I. Libshitz, MD

Multiple Myeloma: Spinal MR Imaging in Patients with Untreated Newly Diagnosed Disease[1]

Spinal magnetic resonance (MR) imaging was performed in 29 patients with newly diagnosed, untreated multiple myeloma. Nineteen (66%) patients were asymptomatic. Sagittal pre- and postcontrast T1-weighted spin-echo images and gradient-recalled-echo images of the thoracic and lumbosacral spine were obtained. Marrow involvement was identified in 20 (69%) patients. There were three MR patterns: focal lesions in nine patients (31%), diffuse involvement in seven (24%), and an inhomogeneous pattern of tiny lesions on a background of normal marrow in four (14%). A statistically significant correlation between MR imaging patterns of marrow involvement and serum hemoglobin values (one-way, $P = .0899$; Kruskal-Wallis, $P = .0620$) and between MR imaging patterns and percentage of marrow plasmacytosis (Kruskal-Wallis, $P = .0314$) was noted, with patterns of diffuse and focal marrow involvement associated with more abnormal values. Spinal MR imaging in patients with early myeloma may reveal marrow involvement in both symptomatic and asymptomatic patients. Some correlation was found between MR imaging patterns and laboratory indexes of disease.

Index terms: Bone marrow, MR, 30.1214 • Myeloma, 30.3452 • Spine, MR, 30.1214 • Spine, primary neoplasms, 30.3452

Radiology 1992; 185:833–840

MULTIPLE myeloma is a monoclonal proliferation of malignant plasma cells that usually affects the bone marrow (1). The peak incidence of multiple myeloma is during the 6th decade of life. It is slightly more common in men and affects three in 100,000 persons per year (1).

The ability of magnetic resonance (MR) imaging to depict bone marrow abnormalities has been documented (2). The purpose of our study was to evaluate spinal MR imaging in patients with newly diagnosed, untreated multiple myeloma to identify and describe patterns of marrow involvement in this largely asymptomatic population. We also attempted to correlate MR imaging patterns of spinal involvement and laboratory parameters to further assess the role of MR imaging in this group of patients.

MATERIALS AND METHODS

Twenty-nine consecutive patients with newly diagnosed, untreated multiple myeloma were studied with MR imaging of the thoracic and lumbosacral spine. There were 13 men and 16 women (age range, 30–76 years; mean, 59 years). Nineteen patients (66%) had no bone pain. Ten patients (34%) reported back pain. Conventional radiographs of the spine were available for evaluation in all patients. Laboratory evaluation for multiple myeloma and posterior iliac crest aspirations was performed in each patient. The extent of tumor mass was staged as high in six patients (hemoglobin level, < 8.5 g/dL [< 85 g/L]; serum calcium level, > 11.5 mg/dL [> 2.87 mmol/L]), low in 14 patients (hemoglobin level, > 10.5 g/dL [> 105 g/L]; serum calcium level, < 11.0 mg/dL [< 2.74 mmol/L]; serum monoclonal component level, < 4.5 g/dL), and intermediate in nine patients (all other cases) (3,4). Three patients (10%) had nonsecretory multiple myeloma with bone marrow plasmacytosis and no evidence of abnormal protein in the blood or urine (5).

MR imaging was performed with a 1.5-T unit (Signa; GE Medical Systems, Milwaukee) with use of a rectangular surface coil. All images were obtained prior to initiation of treatment for multiple myeloma. Sagittal T1-weighted spin-echo (600/20 [repetition time msec/echo time msec]) images were obtained in all patients. Gradient-recalled (GRE) acquisition in the steady state (GRASS; GE Medical Systems) (200–600/13–20; 13°–25° flip angle) images were obtained in 26 patients. GRE images (75/15; 12° flip angle) were obtained in one case. Unenhanced and gadolinium-enhanced T1-weighted images with similar window widths and levels were obtained in 26 patients. T1-weighted MR images of the lumbar and thoracic spine obtained before and after administration of contrast material, viewed with the same window widths and levels in 10 patients with solid primary malignancies, were reviewed to study the presence or lack of enhancement in the uninvolved marrow. All images were acquired in the sagittal plane by using a 256 × 192 or 256 × 128 data acquisition matrix with a 28-cm field of view. Section thickness was 4 mm with a 1-mm intersection gap.

MR images were analyzed for patterns of myelomatous involvement (Figs 1–7). Marrow involvement was characterized as focal when focal areas of fatty marrow replacement with a signal intensity similar to or lower than that of muscle were noted on T1-weighted images in one or more vertebrae (Figs 1, 2, 3, 6). A variegated pattern of involvement was considered to be present when multiple innumerable tiny foci of marrow replacement on a background of uninvolved marrow were observed throughout the spine on T1-weighted images, with subsequent enhancement of these foci on gadolinium-enhanced images (Fig 4). Diffuse involvement was defined as total replacement of fatty marrow throughout the spine on T1-weighted images, with evidence of marrow enhancement on gadolinium-enhanced T1-weighted images (Fig 5). When one or more vertebral bodies were diffusely involved, the pattern of involvement was classified as focal, provided that uninvolved marrow was present in other vertebral bodies. We did not observe more than one pattern of marrow involvement in any one patient in this study.

The number and conspicuity of the le-

Abbreviation: GRE = gradient-recalled.

[1] From the Departments of Diagnostic Radiology (L.A.M., D.G.K.V., N.E.L., E.E.K., H.I.L.), Medical Oncology (M.A.D., R.A.), and Biomathematics (D.A.J.), University of Texas M. D. Anderson Cancer Center, 1515 Holcombe Blvd, Houston, TX 77030. Received February 21, 1992; revision requested May 1; final revision received July 16; accepted July 29. **Address reprint requests to** L.A.M.

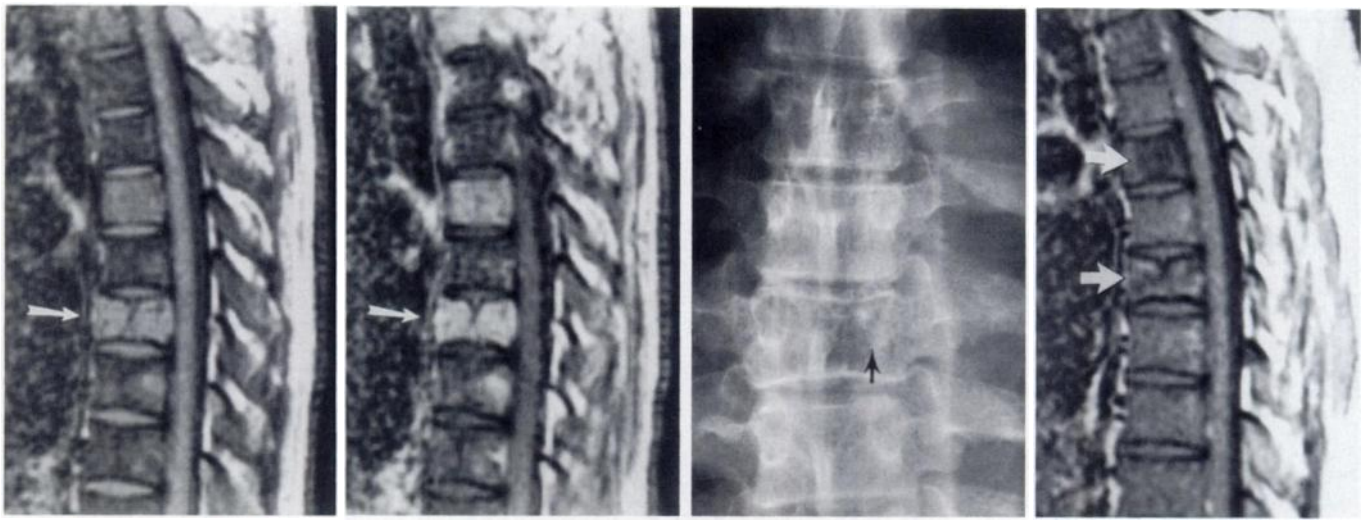

Figure 1. Symptomatic myeloma appearing as a focal pattern of marrow involvement in a 30-year-old man. **(a)** T1-weighted sagittal MR image (600/20) of the thoracic spine reveals an unusual hyperintense appearance of marrow involvement. The seventh dorsal vertebral body is compressed (arrow in **a, b**). There is slight impingement on the thecal sac. **(b)** T1-weighted postcontrast MR image (600/20) reveals enhancement of the lesions. **(c)** Radiograph of the thoracic spine reveals compression and myelomatous lesion in the seventh thoracic vertebral body (arrow). Involvement of the fifth thoracic vertebral body is also noted. **(d)** T1-weighted sagittal MR image (600/20) of the thoracic spine 13 months after treatment reveals focal lesions (arrows) appearing hypointense relative to muscle.

sions with individual sequences were noted. Compression fractures were listed and classified as malignant in pathogenesis when either diffuse or focal and rounded signal intensity abnormality was seen within the marrow. They were considered of benign pathogenesis when either no signal intensity abnormality or a band of low signal intensity parallel to the vertebral end plate was identified on T1-weighted images.

The MR imaging findings were correlated with tumor mass and values of hemoglobin, serum β_2-microglobulin, percentage of bone marrow plasmacytosis, serum creatinine, serum calcium, and serum monoclonal protein. In addition, the type of abnormal protein (immunoglobulin G, 22 patients; immunoglobulin A, four patients; nonsecretory myeloma, three patients) was correlated with MR imaging patterns.

Statistical analysis was performed with the one-way analysis of variance, Kruskal-Wallis one-way analysis of variance by ranks, Student t test, χ^2, and Mann-Whitney test (6). With the small numbers of patients in each MR imaging category the assumption of normality of the means and approximate equality of variances required for the one-way analysis of variance may not hold and are not testable with any degree of power. For this reason, the parametric one-way analysis of variance and the Kruskal-Wallis tests were both performed. When the one-way analysis of variance and the Kruskal-Wallis tests are performed and the data satisfy the assumptions of the one-way analysis of variance, the Kruskal-Wallis test is not as significant as the one-way analysis of variance by 5%–15%, whereas when the one-way analysis of variance assumptions are violated, the Kruskal-Wallis test is more significant.

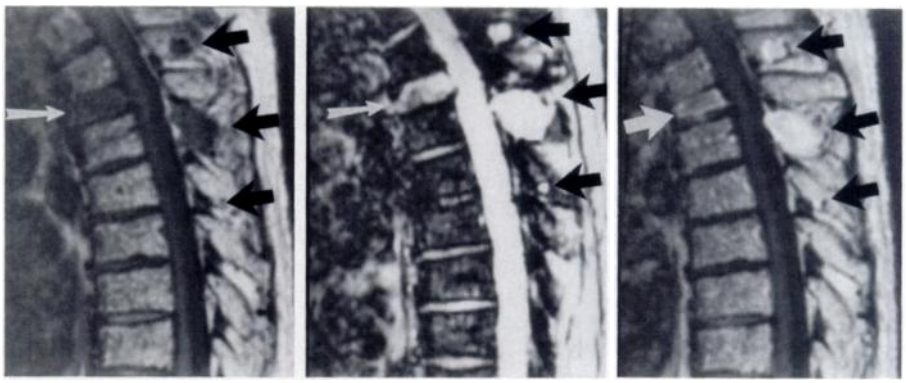

Figure 2. Symptomatic myeloma appearing as a focal pattern of marrow involvement in a 71-year-old man. **(a)** T1-weighted sagittal MR image (600/20) of the thoracic spine shows involvement of the entire compressed third dorsal vertebral body (white arrow in **a–c**) and several focal lesions in the posterior spinal elements (black arrows in **a–c**). **(b)** GRE MR image (217/20; 20° flip angle) better demonstrates the lesions in the posterior spinal elements (black arrows). **(c)** T1-weighted postcontrast image (600/20) reveals enhancement in all areas of marrow involvement. The lesion in the third dorsal vertebra is only faintly seen (white arrow).

RESULTS

Spinal MR imaging revealed marrow involvement in 20 of 29 (69%) patients. Three MR imaging patterns of marrow involvement were noted: focal lesions in nine (31%) patients, diffuse involvement in seven (24%), and a variegated pattern of multiple small lesions on a background of normal marrow in four (14%). In nine (31%) patients, there was no MR imaging evidence of myelomatous involvement. Seven patients with focal lesions, two patients with diffuse involvement, and one patient with a variegated pattern reported back pain. All patients with a normal MR imaging study were free of bone pain.

There were 66 focal lesions (lumbosacral spine [n = 30]; thoracic spine [n = 36]). Only 12 (18%) lesions were demonstrated as lytic foci on conventional radiographs. On T1-weighted images, 52 lesions (79%) were hypointense relative to muscle, whereas 14 (21%) lesions, all in one patient, were hyperintense relative to muscle (Fig 1). Conventional radiographs of the spine in this patient revealed lytic lesions consistent with multiple myeloma. On follow-up MR images of the spine 13 months after initiation of treatment, the focal lesions were hypointense relative to muscle, suggesting the presence of hemorrhage on

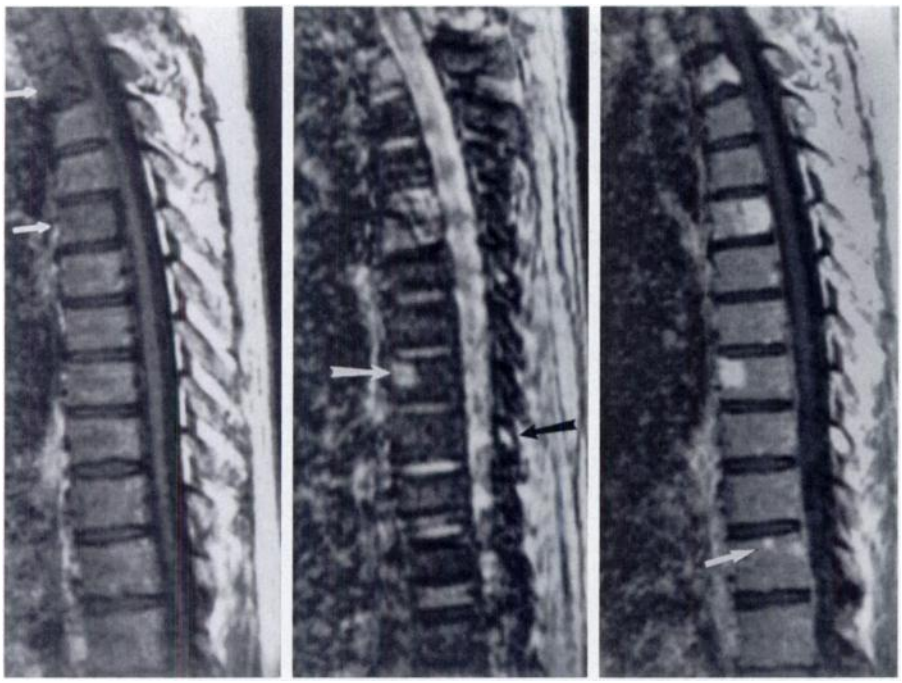

a. b. c.

Figure 3. Symptomatic myeloma appearing as a focal pattern of marrow involvement in a 48-year-old man. **(a)** T1-weighted sagittal MR image (600/20) of the thoracic spine reveals focal areas of decreased signal intensity (arrows). **(b)** GRE image (75/15; 12° flip angle) better demonstrates the lesions and reveals two additional lesions in the spinous process of the ninth vertebral body (black arrow) and in the body of the eighth dorsal vertebra (white arrow). **(c)** T1-weighted postcontrast image (600/20) clearly demonstrates the lesions and reveals an additional small lesion in the 11th dorsal vertebral body (arrow).

the initial study. On GRE images, all visualized lesions were hyperintense relative to muscle. All 37 lesions studied after contrast enhancement revealed various degrees of uptake of contrast material.

Nineteen (39%) of the 49 lesions studied with both T1-weighted and GRE sequences were equally well seen on both series. Eleven (22%) lesions were better seen on T1-weighted images. GRE images better depicted 11 (22%) lesions, six of which were located in the posterior spinal elements (Fig 2). Eight (16%) lesions identified on T1-weighted images were not seen on GRE images. Eleven (30%) of 37 lesions studied with pre- and postcontrast T1-weighted images could be identified only on the unenhanced images, whereas five (14%) lesions in a patient with a paucity of fatty marrow in the spine were better seen on the enhanced images (Fig 3).

In five of eight patients studied with both T1-weighted and GRE sequences, T1-weighted images better demonstrated focal lesions. In two of eight patients, focal lesions were equally well seen with both sequences, while in one patient with a relative lack of spinal fatty marrow, focal lesions were better seen on GRE images. Focal lesions were better depicted on unenhanced T1-weighted images compared with gadolinium-enhanced images in five of seven patients studied with both sequences, equally well seen in one patient, and less well visualized in one patient with a paucity of spinal fatty marrow. GRE images were superior in demonstrating focal lesions in five of six patients studied with both GRE and gadolinium-enhanced images. In one patient, both series failed to reveal any of the lesions noted on the unenhanced T1-weighted images.

Follow-up MR imaging studies were performed in three patients with focal lesions 6–13 months after initiation of treatment; marked improvement was noted in two, and in another patient, who had nonsecretory myeloma, no change was noted.

The variegated pattern was noted on T1-weighted images as multiple tiny foci hypointense relative to uninvolved marrow that enhanced on gadolinium-enhanced T1-weighted images (Fig 4). Multiple hyperintense foci of marrow involvement were noted in only one of three patients studied with GRE imaging. Follow-up MR imaging 38 months later revealed marked progression of the variegated pattern in one patient with low tumor mass myeloma who never received treatment and remained asymptomatic. A 6-month follow-up MR imaging study after treatment in a patient with intermediate tumor mass revealed marked interval improvement in the appearance of the variegated pattern (Fig 4).

In seven patients with diffuse involvement of the marrow, T1-weighted images revealed lack of fatty marrow in the spine, with the intervertebral disks being iso- or hyperintense relative to the abnormal vertebrae (Fig 5). The signal intensity of the marrow was slightly lower than that of adjacent muscle groups. A diffuse increase in signal intensity was noted in only two of six cases studied with GRE imaging (Fig 5). Gadolinium-enhanced images revealed diffuse enhancement of the marrow in all cases, with the disks becoming hypointense relative to the vertebral bodies (Fig 6). Follow-up MR imaging 1 month after bone marrow transplantation in one patient with diffuse marrow involvement revealed an almost normal appearance of the marrow with no definite evidence of enhancement.

A retrospective review of pre- and postcontrast T1-weighted images in 10 patients with solid primary malignancies, viewed with similar window widths and levels, did not reveal any change in the appearance of uninvolved vertebral bodies and relative signal intensities of the intervertebral disks after administration of contrast material.

Twenty-eight compression fractures were observed in 13 patients (11 [39%] of the lumbosacral spine; 17 [61%] of the thoracic spine). Twenty-two (79%) were considered of malignant pathogenesis on MR images (Figs 1, 2, 4, 6). Lytic lesions were identified in four (14%) compressed vertebral bodies on conventional radiographs of the spine. Six (21%) of the 28 compression fractures showed no evidence of myelomatous involvement on MR images (Fig 7).

Statistical correlation of the MR imaging patterns with hemoglobin values revealed a marginally significant relationship by means of one-way ($P = .0899$) and Kruskal-Wallis ($P = .0620$) analysis, with the diffuse and focal lesion patterns associated with lower hemoglobin values than the variegated and normal patterns (Table 1). A graphic illustration of these observations is presented in Figures 8 and 9. The relationship between MR imaging patterns and bone marrow plasmacytosis was not significant at one-way analysis ($P = .14$) but was

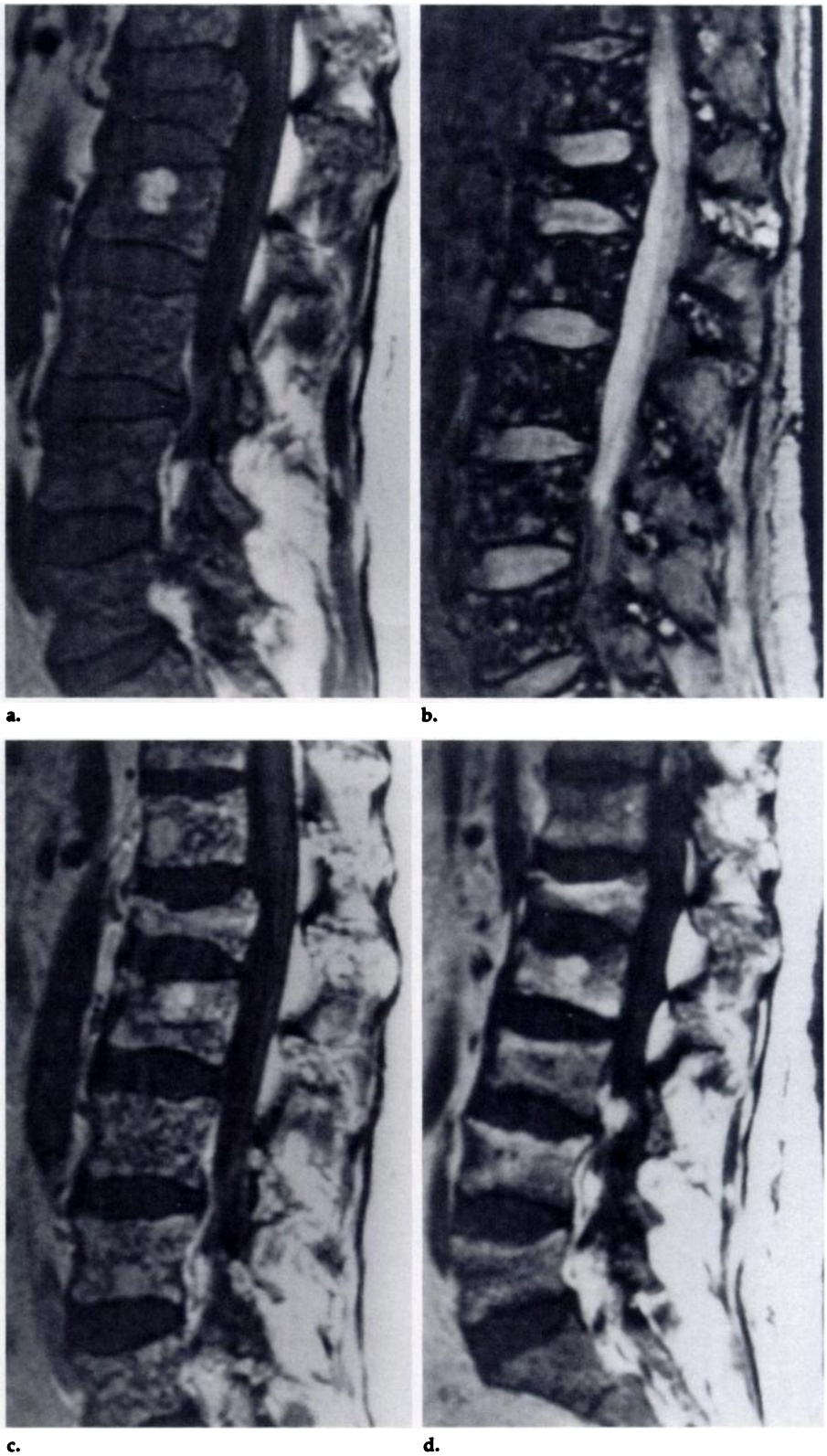

Figure 4. Symptomatic myeloma appearing as a variegated pattern of marrow involvement in a 45-year-old man. **(a)** T1-weighted sagittal image (600/20) of the lumbar spine reveals a variegated appearance of the marrow. The hyperintense focus in the second lumbar vertebral body is an area of focal fatty marrow. The first lumbar vertebra is compressed, with retropulsion of tumorous bone. **(b)** GRE sagittal MR image (650/20; 20° flip angle) reveals multiple hyperintense foci of disease throughout the lumbar spine. Note involvement of the posterior spinal elements. **(c)** T1-weighted postcontrast image (600/20) reveals inhomogeneous enhancement throughout the lumbar spine. **(d)** T1-weighted sagittal image (600/20) of the lumbar spine 6 months after treatment reveals an increase in the fatty marrow content of the spine. Several vertebral compression fractures have developed.

significant at Kruskal-Wallis analysis ($P = .0314$); MR imaging evidence of marrow involvement was associated with higher values of bone marrow plasmacytosis. A significant relationship between MR patterns and serum β_2-microglobulin, monoclonal protein, serum creatinine, and serum calcium was not observed with either test. No correlation was found between types of abnormal protein and MR imaging patterns.

Table 2 shows the relationship between tumor mass and MR imaging patterns. There were no high-tumor-mass variegated or normal MR imaging patterns. If the Table is collapsed by combining intermediate and low tumor mass and compared with combined diffuse and focal patterns versus normal and variegated patterns, the resultant χ^2 is 6.15 ($P = .013$), indicating a potential relationship between tumor mass and MR imaging patterns.

As the number of patients in individual groups was small and because the statistical analysis revealed a tendency for diffuse and focal lesion patterns to be associated with more pronounced laboratory abnormalities and higher tumor mass, diffuse and focal lesion patterns were pooled into a single group and variegated and normal patterns, into a second group. Statistical analysis with the Student *t* test revealed significantly lower values of hemoglobin ($P = .024$) and significantly higher values of bone marrow plasmacytosis ($P = .029$) for the diffuse and focal lesion group in comparison with the variegated and normal group. Mann-Whitney nonparametric tests corroborated the association of MR imaging patterns and bone marrow plasmacytosis ($P < .01$) but not the association of MR imaging patterns and hemoglobin ($P = .21$), indicating the need for further studies with larger numbers of patients in individual groups.

DISCUSSION

In multiple myeloma, plasma cell infiltration of the marrow occurs in both a nodular and interstitial fashion (7). Therefore, various patterns of involvement are expected on MR images of the spine. In our study, spinal MR imaging revealed three patterns of myelomatous involvement of the marrow in 20 of 29 (69%) patients. In agreement with other authors, we saw that focal areas of marrow in-

Table 1
MR Imaging Pattern versus Laboratory Parameters

MR Imaging Pattern	No. of Patients	Hemoglobin (g/dL [g/L])	β_2-Microglobulin (mg/L [nmol/L])	Monoclonal Component (g/L)	Bone Marrow Plasmacytosis (%)	Calcium (mg/dL [mmol/L])	Creatinine (mg/dL [μmol/L])
Focal	9	10.7 ± 2.0 (107 ± 20)	4.8 ± 5.1 (407 ± 432)	4.4 ± 3.6	46.5 ± 31.2	9.8 ± 1.1 (2.45 ± 0.27)	1.3 ± 0.8 (110 ± 70)
Diffuse	7	9.3 ± 2.7 (93 ± 27)	7.7 ± 8.5 (653 ± 720)	3.8 ± 3.0	41.4 ± 23.9	10.0 ± 1.7 (2.50 ± 0.42)	1.2 ± 0.4 (110 ± 40)
Variegated	4	11.9 ± 0.3 (119 ± 3)	3.5 ± 1.8 (297 ± 153)	3.4 ± 2.3	34.7 ± 11.3	8.7 ± 0.1 (2.17 ± 0.02)	1.1 ± 0.4 (100 ± 40)
Normal	9	11.6 ± 1.6 (116 ± 16)	3.1 ± 1.1 (263 ± 93)	3.2 ± 1.1	20.3 ± 18.6	9.4 ± 0.5 (2.35 ± 0.12)	1.1 ± 0.3 (100 ± 30)

Note.—Values are the mean ± 1 standard deviation. Values in parentheses are expressed in SI units.

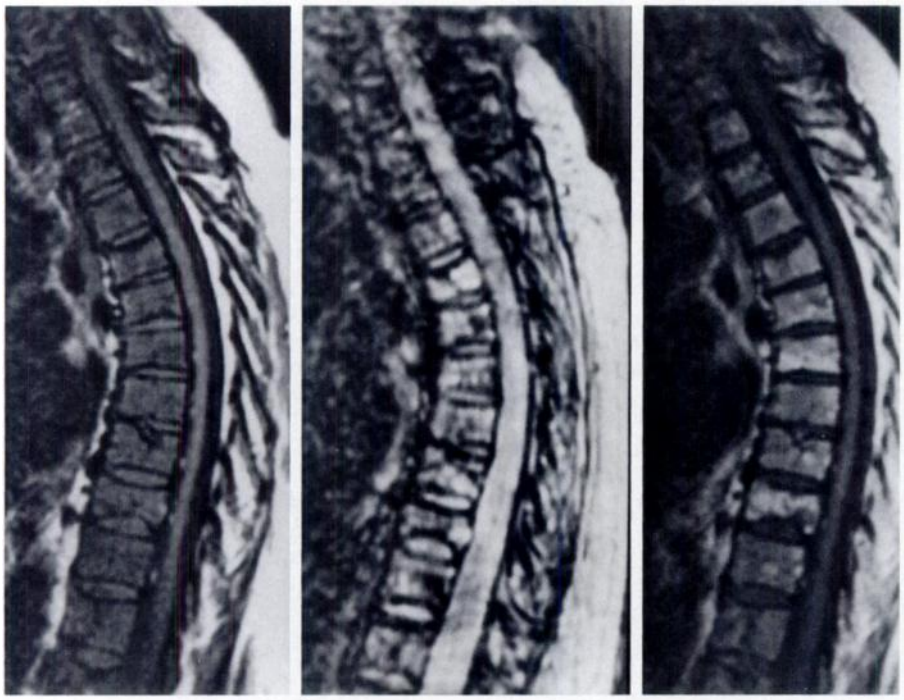

a. **b.** **c.**

Figure 5. Symptomatic myeloma appearing as a diffuse pattern of marrow involvement in a 56-year-old woman. **(a)** T1-weighted sagittal MR image (600/20) of the thoracic spine reveals complete replacement of the fatty marrow. Note the isointense appearance of vertebral bodies relative to intervertebral disks. **(b)** GRE image (250/20, 20° flip angle) reveals diffuse inhomogeneous signal hyperintensity throughout the thoracic spine. **(c)** T1-weighted postcontrast image (600/20) reveals diffuse enhancement of the marrow. The intervertebral disks are now hypointense relative to the enhanced vertebral bodies.

volvement were the most frequently observed abnormality (8–10) (Fig 1). In addition, total marrow replacement (diffuse pattern) and inhomogeneous marrow replacement (variegated pattern) were noted in seven (24%) and four (14%) patients, respectively.

All three patterns of marrow involvement were seen on T1-weighted MR images. Both variegated and diffuse patterns, however, when noted on T1-weighted images, had to be differentiated from normal patterns of inhomogeneous distribution of fatty marrow often observed in older persons or from the persistent red marrow pattern occasionally seen in younger patients with myeloma (11). Gadolinium-enhanced T1-weighted images showed diffuse or inhomogeneous enhancement, respectively, in all patients with diffuse or variegated involvement of the marrow.

To our knowledge, gadopentetate dimeglumine has not been previously employed in the evaluation of myelomatous involvement of the spine. Although normal marrow may markedly enhance in children younger than 7 years, enhancement of the marrow is subtle in adults and can be appreciated only when intensity measurements are calculated (12,13). Intervertebral disks are isointense relative to spinal marrow in patients with diffuse marrow involvement. After administration of contrast material, the disks become hypointense relative to marrow as the abnormal vertebral bodies enhance.

GRE images were not helpful in depicting diffuse or variegated marrow involvement. On GRE images, bone is markedly hypointense to muscle, and in the majority of cases, neoplastic aggregates will appear as hyperintense foci; it is possible that a diffuse or variegated pattern of plasma cell infiltration of the marrow may not produce sufficient increase in cellularity to overcome the magnetic susceptibility effect of bone with a GRE sequence (14). Spin-echo T2-weighted or inversion recovery images, though more time-consuming, may be more sensitive in depicting these patterns (10).

In our study, focal lesions were better seen on T1-weighted images in the majority of cases. GRE images were useful in depicting lesions in the posterior elements by suppressing the subcutaneous fat and thus increasing contrast between lesion and background. In patients with relatively little fatty spinal marrow and poor lesion-to-marrow contrast on T1-weighted images, both GRE and enhanced T1-weighted images clearly depicted the marrow involvement. GRE images failed to demonstrate 16% of focal lesions noted on T1-weighted images.

The "masking" effect of gadopentetate dimeglumine on the MR imaging appearance of marrow lesions has been previously stressed (15). In our study, 30% of focal lesions could not be detected on the enhanced images because they became isointense relative to uninvolved marrow. In one patient, a solitary focal lesion could not be identified on the

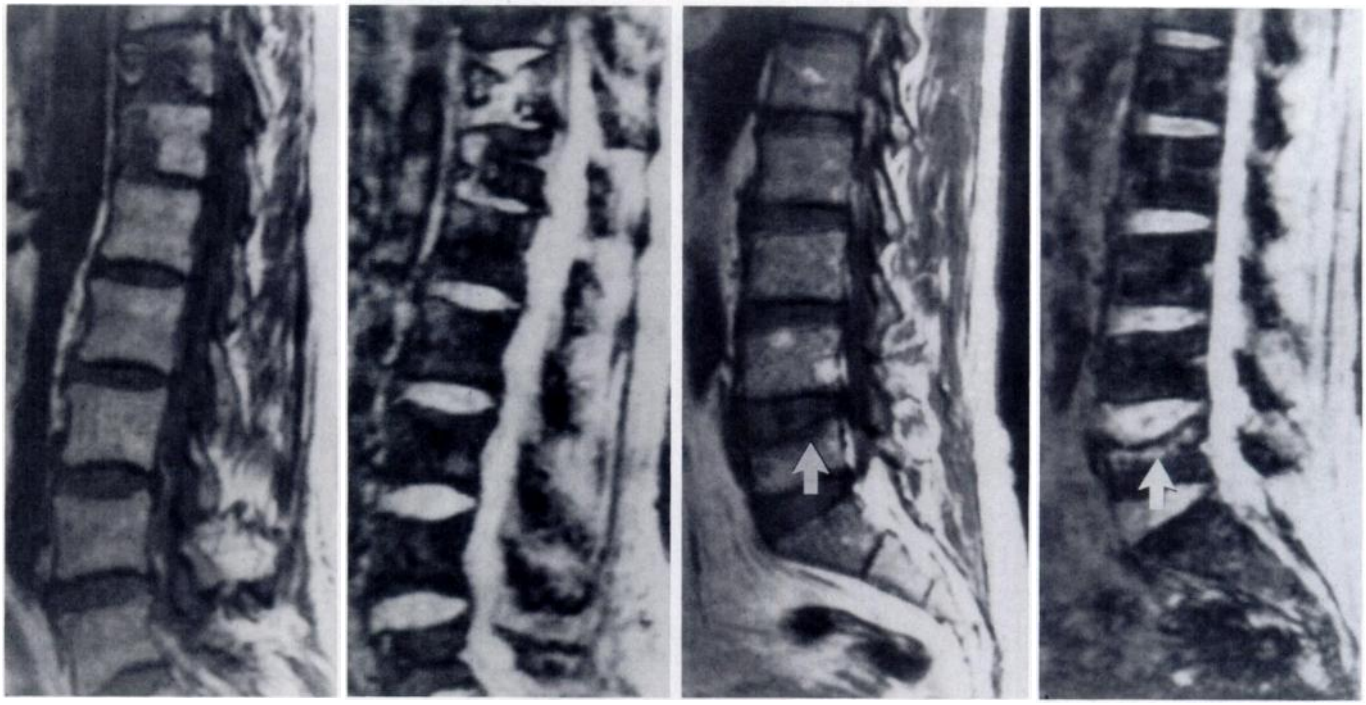

6a. 6b. 7a. 7b.

Figures 6, 7. **(6)** Malignant compression fractures in a 63-year-old woman with symptomatic myeloma. **(a)** T1-weighted sagittal image (600/20) of the lumbar and lower thoracic spine reveals compression fractures of the 11th and 12th dorsal vertebrae, with focal marrow-replacing lesions. **(b)** GRE MR image (300/20; 20° flip angle) shows an increase in the signal intensity of the focal marrow involvement in the 11th and 12th vertebral bodies. **(7)** Asymptomatic myeloma and an acute benign compression fracture in a 55-year-old man. **(a)** T1-weighted sagittal MR image (600/20) of the lumbar spine reveals compression of the fifth lumbar vertebra, with a hypointense band adjacent to the superior end plate (arrow). Focal areas of fatty marrow are noted in the L-4 and L-1 vertebral bodies. **(b)** GRE MR image (267/20; 20° flip angle) reveals an increase in the signal intensity of the band of signal alteration in the fifth lumbar vertebra noted in a (arrow).

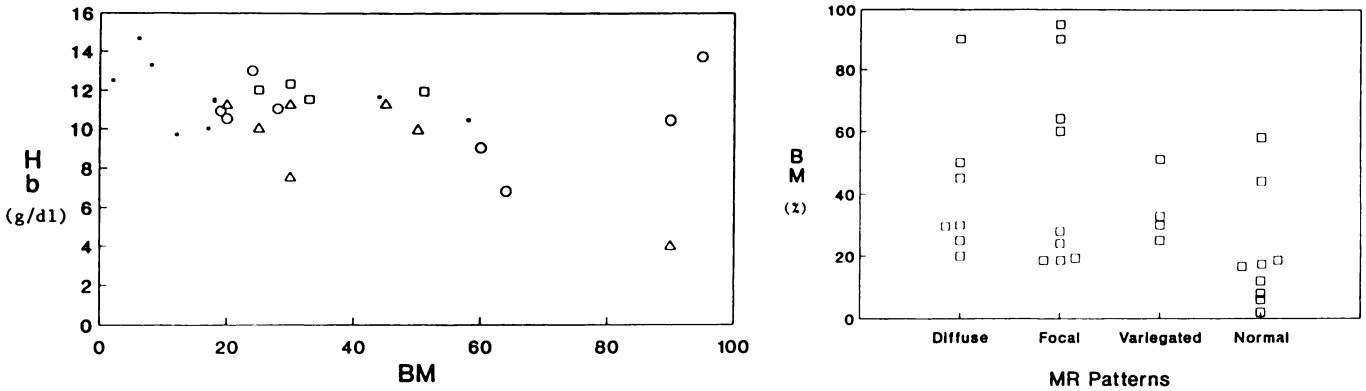

8. 9.

Figures 8, 9. **(8)** Graph shows MR imaging patterns versus hemoglobin level (*Hb*) and bone marrow plasmacytosis (*BM*), expressed as a percentage. △ = diffuse pattern, ○ = focal pattern, □ = variegated pattern, ■ = normal pattern. **(9)** Graph shows MR imaging patterns versus bone marrow plasmacytosis (*BM*), expressed as a percentage.

gadolinium-enhanced images. Other authors have reported focal lesions in myeloma to be better or exclusively seen on T2-weighted MR images (10).

An unusual finding in this study was the hyperintense appearance of the focal lesions relative to muscle and disk in a 30-year-old patient with myeloma (Fig 1). Amyloid deposition was initially considered a possible pathogenesis of this finding; in a case of amyloid deposition in the spine reported in the literature, however, the abnormality was seen as a decrease in the signal intensity of the spinal marrow relative to the intervertebral disks on T1-weighted images (16). Resolution of the hyperintense signal with a hypointense appearance of the focal lesions relative to muscle on a 13-month follow-up MR imaging study of the spine suggested the presence of hemorrhage within foci of myelomatous involvement of the marrow at the time of the initial study (17). Conventional radiographs obtained in this patient revealed lytic lesions consistent with myeloma. Radiologists should be aware that lesions that are hyperintense relative to marrow on T1-weighted MR images of the spine do not always indicate benign pathogenesis such as those of hemangiomas or focal fatty islands and may rarely be encountered in patients with myeloma (18).

Several MR imaging criteria have been employed to differentiate benign from malignant compression

Table 2
MR Imaging Pattern versus Tumor Mass

Tumor Mass	MR Imaging Pattern				
	Diffuse	Focal	Variegated	Normal	Total
High	3	3	0	0	6
Intermediate	2	2	1	4	9
Low	2	4	3	5	14
Total	7	9	4	9	29

fractures (19,20). Absence of marrow signal alteration has been reported to indicate a benign vertebral compression fracture (20). On spin-echo MR images, diffuse marrow replacement involving the entire vertebral body in a compressed vertebra has been described as highly suggestive of a malignant pathogenesis (19). Diffuse involvement, however, was noted in only eight of 28 (29%) compression fractures in this study. In half of the 28 compression fractures, a focal or variegated pattern of marrow involvement was noted.

In a recently reported study, only two of 38 (5%) compressions had complete replacement of the marrow by myeloma and 17 of 38 (45%) showed lesser extent of marrow involvement (10). Therefore, in multiple myeloma, a vertebral compression fracture may occur without the MR imaging observation of marrow being totally replaced by tumor cells, possibly because, in addition to tumorous marrow infiltration, osteoclast activating factors also contribute to the development of vertebral compression fractures (1). In such cases, the configuration of the marrow abnormality (rounded focal versus parallel to endplate band) will aid in differentiating a malignant from a benign fracture (20) (Figs 6, 7). As previously noted, at spinal MR imaging in patients with malignancies other than myeloma, enhanced images do not always help in evaluating the nature of compression fractures because enhancement may occur in malignant as well as in posttraumatic fractures, depending on the age of the fracture (21,22).

An important finding in our study was the correlation between MR imaging patterns of marrow involvement and hemoglobin and bone marrow plasmacytosis values: The diffuse and focal lesion patterns were associated with more pronounced laboratory abnormalities. In evaluating these results, one must keep in mind that hemoglobin and bone marrow plasmacytosis more closely reflect the status of the marrow than do other laboratory parameters (23). At our institution, patients with indolent myeloma (asymptomatic, low tumor mass) do not receive treatment until they become symptomatic or their disease proceeds to a higher tumor stage. Preliminary results of a prospective clinical study show that patients with indolent myeloma and focal or diffuse involvement noted on MR images of the spine needed treatment earlier than did patients with a variegated or normal MR imaging appearance of the spine. Libshitz et al (10) found no correlation between MR imaging appearances and serum β_2-microglobulin or monoclonal protein values in 32 patients with multiple myeloma; this is in agreement with our results. They also, however, noted no relationship between MR imaging appearances and bone marrow plasmacytosis, possibly because different criteria were employed for MR imaging pattern characterization (10). Long-term prospective studies are required to establish the significance and prognostic value of the different MR imaging patterns of marrow involvement.

Return of marrow appearance to normal on spinal MR images a month after bone marrow transplantation in one patient correlated with lack of plasmacytosis on a marrow aspirate, suggesting a potential role of MR imaging in evaluating response to treatment.

Nonsecretory myeloma is characterized by involvement of the bone marrow but no evidence of abnormal protein in the blood or urine (5). In nonsecretory myeloma (three of 29 patients in this series), assessment of the clinical course depends on repeated marrow aspirations because there is no detectable monoclonal peak in the serum (5). An iliac aspirate may not always be representative of the marrow involvement due to both nodular and interstitial tumor growth patterns (7). MR imaging may prove to be a useful, noninvasive method of assessing the course of disease in these patients.

In summary, spinal MR imaging may reveal marrow involvement (focal, diffuse, or variegated) in both symptomatic and asymptomatic patients with multiple myeloma. T1-weighted images should be obtained in all patients. Enhanced T1-weighted images can be of great value in cases of diffuse or variegated involvement. GRE images may be employed in addition to T1-weighted images in selected cases of focal lesions (posterior elements, paucity of fatty marrow). MR imaging findings of marrow involvement do correlate with certain laboratory indexes of tumor burden, with diffuse involvement and focal lesions tending to occur in patients with more advanced disease. MR imaging appears promising for assessing response to treatment, especially in patients with nonsecretory myeloma. Long-term prospective studies may be helpful in defining the prognostic value of MR imaging patterns in patients with multiple myeloma. ■

Acknowledgments: The assistance provided by Debbie Smith and Mary Carr in the preparation of this manuscript is gratefully acknowledged. We thank Dana Holloway, Brenda Hutsko, Ricardo Estrada, and Joseph Kurian for technical assistance and Glenda Deal for secretarial assistance.

References

1. Longo DL. Plasma cell disorders. In: Wilson JD, Braunwald E, Isselbacher KJ, et al, eds. Harrison's principles of internal medicine. 12th ed. New York: McGraw-Hill, 1991; 1412–1416.
2. Vogler JB III, Murphy WA. Bone marrow imaging. Radiology 1988; 168:679–693.
3. Alexanian R, Barlcerzak S, Bonnett JD, et al. Prognostic factors in multiple myeloma. Cancer 1975; 36:1192–1201.
4. Durie BGM, Salmon SE. A clinical staging for multiple myeloma. Cancer 1975; 36:842–854.
5. Dreicer R, Alexanian R. Nonsecretory myeloma. Am J Hematol 1982; 13:313–316.
6. Norusis Marija J. SPSS/PC + 4.0. Chicago: SPSS, 1991.
7. Barti R, Frisch B, Diem H, et al. Bone marrow histology and serum beta 2 microglobulin in multiple myeloma: a new prognostic strategy. Eur J Haematol 1989; 43(suppl 51):88–98.
8. Daffner RH, Lupetin AR, Dash N, et al. MRI in the detection of malignant infiltration of bone marrow. AJR 1986; 146:353–358.
9. Fruehwald FXJ, Tscholakoff D, Schwaighofer B, et al. Magnetic resonance imaging of the lower vertebral column in patients with multiple myeloma. Invest Radiol 1988; 23:193–199.
10. Libshitz HI, Malthouse SR, Cunningham D, et al. Magnetic resonance appearance of multiple myeloma. Radiology 1992; 182: 833–837.
11. Ricci C, Cova M, Kang YS, et al. Normal age-related patterns of cellular and fatty bone marrow distribution in the axial skel-

eton: MR imaging study. Radiology 1990; 177:83–88.
12. Breger RK, Williams AL, Daniels DL, et al. Contrast enhancement in spinal cord imaging. AJR 1989; 153:387–391.
13. Sze G, Bravo S, Baierl P, Shimkin PM. Developing spinal column: gadolinium-enhanced MR imaging. Radiology 1991; 180: 497–502.
14. Czervionke LF, Daniels DL, Wehrli FW, et al. Magnetic susceptibility aftifacts in gradient-recalled echo MR imaging. AJNR 1988; 9:1149–1155.
15. Sze G. Gadolinium-DTPA in spinal disease. Radiol Clin North Am 1988; 26:1009–1024.
16. Olliff JFC, Hardy LR, Williams MP, et al. Case report: magnetic resonance imaging of spinal amyloid. Clin Radiol 1989; 40:632–633.
17. Atlas SW, Grossman RI, Gomori JM, et al. Hemorrhagic intracranial malignant neoplasms: spin-echo MR imaging. Radiology 1987; 164:71–77.
18. Ross JS, Masaryk TJ, Modic MT, Carter JR, Mapstone T, Dengel FH. Vertebral hemangiomas: MR imaging. Radiology 1987; 165:165–169.
19. Baker LL, Goodman SB, Perkash I, Lane B, Enzmann DR. Benign versus pathologic compression fractures of vertebral bodies: assessment with conventional spin-echo, chemical shift, and STIR MR imaging. Radiology 1990; 174:495–502.
20. Yuh WTC, Zachar CK, Barloon TJ, Sato Y, Sickels WJ, Hawes DR. Vertebral compression fractures: distinction between benign and malignant causes with MR imaging. Radiology 1989; 172:215–218.
21. Staebler A, Gaertner C, Seiderer M, et al. Differential diagnosis of benign and malignant vertebral compression fractures with MR imaging: use of antiphased long-TR gradient-echo sequences and Gd-DTPA and STIR sequences (abstr). Radiology 1991; 181(P):203.
22. Baker LL, Gean-Marton AD, Koeller KK, et al. Compressed vertebral body: MR imaging features in trauma, osteopenia, infection and tumor (abstr). Radiology 1991; 181(P):203.
23. Alexanian R, Barlogie B, Fritsche H. Beta 2 microglobulin in multiple myeloma. Am J Hematol 1985; 20:345–351.